Phase diagram and momentum distribution of an interacting Bose gas in a bichromatic lattice

Xiaolong Deng,[1] R. Citro,[1,2,*] A. Minguzzi,[1,†] and E. Orignac[3]
[1]*Laboratoire de Physique et Modélisation des Mileux Condensés, Université Joseph Fourier, CNRS Boîte Postale 166, 38042 Grenoble, France*
[2]*Dipartimento di Fisica E.R. Caianiello and C.N.I.S.M., Universitá di Salerno, via S. Allende, 84081 Baronissi, Salerno, Italy*
[3]*Laboratoire de Physique de l'École Normale Supérieure de Lyon, Université de Lyon, CNRS UMR5672, 46 Allée d'Italie, 69364 Lyon Cedex 07, France*
(Received 20 March 2008; published 21 July 2008)

We determine the phase diagram and the momentum distribution for a one-dimensional Bose gas with repulsive short-range interactions in the presence of a two-color lattice potential, with an incommensurate ratio among the respective wavelengths, by using a combined numerical (density matrix renormalization group) and analytical (bosonization) analysis. The system displays a delocalized (superfluid) phase at small values of the intensity of the secondary lattice V_2 and a localized (Bose-glasslike) phase at larger intensity V_2. We analyze the localization transition as a function of the height V_2 beyond the known limits of free and hard-core bosons. We find that weak repulsive interactions disfavor the localized phase, i.e., they increase the critical value of V_2 at which localization occurs. In the case of integer filling of the primary lattice, the phase diagram at fixed density displays, in addition to a transition from a superfluid to a Bose glass phase, a transition to a Mott-insulating state for not too large V_2 and large repulsion. We also analyze the emergence of a Bose-glass phase by looking at the evolution of the Mott-insulator lobes when increasing V_2. The Mott lobes shrink and disappear above a critical value of V_2. Finally, we characterize the superfluid phase by the momentum distribution, and show that it displays a power-law decay at small momenta typical of Luttinger liquids, with an exponent depending on the combined effect of the interactions and of the secondary lattice. In addition, we observe two side peaks that are due to the diffraction of the Bose gas by the second lattice. This latter feature could be observed in current experiments as characteristics of pseudo-random Bose systems.

DOI: 10.1103/PhysRevA.78.013625 PACS number(s): 03.75.Lm, 71.23.An, 68.65.Cd

I. INTRODUCTION

The interplay between disorder and interactions has been a long-standing challenge for condensed-matter theory. In the absence of interactions, a random potential can induce Anderson localization [1], i.e., make all the single-particle eigenstates localized. In the absence of disorder, bosons on a lattice with repulsive interactions display, for commensurate filling, a superfluid (SF) to Mott insulator (MI) transition as the repulsion is increased [2], with the superfluid phase displaying large density fluctuations and a gapless excitation spectrum, while the Mott phase is incompressible and has a gap in the excitation spectrum. If one considers both repulsive interactions and disorder, these two effects will compete: while disorder makes the bosons localized, short-range repulsive interaction energy increases as the square of boson density and hence the total energy of the system is minimized by depleting the localized condensate toward a more uniform density distribution. As a result, in a lattice Bose gas with short-range interactions, a novel Bose-glass (BG) phase, nonsuperfluid yet compressible, emerges between the superfluid and the Mott insulator. This phase was first predicted for one-dimensional systems [3], and later, building on the one-dimensional analysis, this prediction was extended to two- and three-dimensional systems [2]. From the experimental point of view, it is possible to realize a system of bosons in a random potential by placing ^{4}He in porous media such as Vycor, aerogels, or xerogels [4,5], or by using artificially disordered Josephson junction networks [6]. Experiments in porous media revealed that the critical exponents of the normal-superfluid transition in helium were different from those in pure helium in the case of aerogels and xerogels. However, the aerogel and xerogel structures can hardly be described by a short-range correlated random potential. In the case of Josephson junctions, localization of vortices was observed, but because of dissipation, this system cannot be treated as fully coherent. The phase diagram of a disordered boson system has also been intensively studied by quantum Monte Carlo simulations [7–10]. While some conjectures made in Ref. [2]. could be confirmed, it appeared that very large system sizes were required to obtain reliable results. Due to the theoretical difficulty of the problem, one approach has been to reduce the spatial dimensionality. In one dimension, it is known that in the absence of interactions, all states are localized as soon as the random potential is nonzero [11,12]. Moreover, powerful specific techniques are available to handle the interactions; this is the case, e.g., of the bosonization technique [13] or of the density matrix renormalization group (DMRG) method [14,15]. For the specific case of a one-dimensional Bose gas subjected to an uncorrelated disorder (in the absence of a lattice), the phase diagram has been obtained by Giamarchi and Schulz [3], showing that while for zero interactions the system is always localized, for nonzero values of the repulsive interactions a superfluid phase is possible at small values of disorder. Reference [3]. also predicted that the nonsuperfluid (Bose-glass) phase

*citro@sa.infn.it
†anna.minguzzi@grenoble.cnrs.fr

 ©2008 The American Physical Society

of an interacting Bose gas is expected to differ markedly from the noninteracting Anderson-localized (AG) phase, e.g., the density profile of a Bose glass phase is rather uniform, in contrast to the highly inhomogeneous density profile of an ideal Bose gas in a disordered potential where all the particles occupy the lowest single-particle localized orbital. The phase diagram of a disordered, interacting Bose gas in one dimension has been the subject of several numerical investigations by quantum Monte Carlo methods [16,17], strong-coupling expansions [18], and DMRG approaches [19], which have established the existence of a Mott insulating phase separated from the superfluid phase by a Bose glass phase for disorder not excessively strong. For stronger disorder, these numerical studies have established that only the Bose glass and the superfluid is present. Also, the existence of a superfluid dome in the phase diagram has been obtained for the incommensurate case [19].

With the development of atom cooling and trapping techniques, studying the Mott transition of bosons has become experimentally feasible [20]. Moreover, recent experiments with ultracold atomic gases have realized a pseudodisordered potential by superimposing two optical lattices with an incommensurate ratio between their spatial periodicities [21] in a regime where interactions are important. Experimentally, it is possible to characterize the system by measuring the excitation spectrum, the momentum distribution, and higher-order (e.g., noise) correlations functions, as well as by looking at the equivalent of transport behavior through the study of the damping of large-amplitude dipole oscillations [22].

While the experiments performed with a bichromatic lattice were focused on a regime where the lattice acts as a disorder potential, the physics of a bichromatic lattice is much richer, and the aim of this work is to describe the different possible phases of an interacting Bose gas subjected to such lattices. In the absence of interaction, the Schrödinger equation in a bichromatic potential treated in the tight-binding approximation is known as the Harper model or the "almost Mathieu problem" and has been extensively studied by solid-state physicists [23,24] and mathematical physicists [25]. It is known to display a delocalized regime for weak incommensurate potential and a localized regime for strong incommensurate potential, the two regimes being related by a duality transformation. In the limit of infinitely strong repulsions among the bosons (the so-called Tonks-Girardeau regime), the problem can be solved by mapping to an ideal spinless Fermi gas subjected to the same external potential [26]. In particular, the model displays the same localization-delocalization threshold as in the noninteracting case. However, the momentum distribution of the Tonks-Girardeau bosons is not directly related to that of the spinless fermions, and for the specific case of the bichromatic potential it has been studied in [27]. The case of spinless fermions (or hard-core bosons) with nearest-neighbor repulsion was studied in [28]. We focus here on the regime of intermediate repulsive interaction strengths. In the case of commensurate filling of the primary lattice and for $\Delta=0$ (where Δ measures the strength of the secondary lattice potential), a Mott-insulator phase is expected to occur at large values of interaction strengths $U_c/t \simeq 3.3$ [30], where U_c is the critical on-site repulsion and t is the hopping matrix element. In the disordered case, this Mott-insulating phase competes with the localized phase, and is expected to induce a Bose-glass intermediate phase.

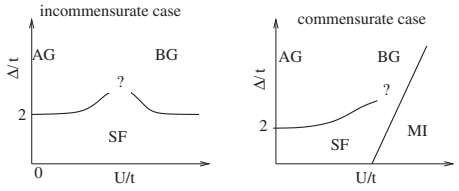

FIG. 1. Schematic representation of the expected phase diagram for a Bose gas subjected to a bichromatic potential. "AG" is the Anderson-localized inhomogeneous phase, "BG" is the Bose-glass phase, "SF" is the nonlocalized superfluidlike phase (i.e., displaying power-law decay of the phase-phase correlation function), and "MI" is the Mott-insulator phase. The "?" sign stands for the region that need to be numerically investigated.

A Bose gas subjected to a quasiperiodic potential with finite interaction strengths has been previously studied by Roth *et al.* [31] by exact diagonalization on a very small system and by Roscilde [32] in the case of a specific choice of the height of the secondary lattice. In the present paper, we use a combination of DMRG methods and low-energy bosonization techniques to infer the phase diagram of the gas at varying height of the secondary lattice and interaction strengths, both for the case of integer and noninteger filling of the main lattice. The schematic summary of the known limits of the phase diagram is presented in Fig. 1. One of our aims is to see how the Mott lobes are modified by the presence of the secondary lattice in the commensurate case and to establish a phase diagram for both the commensurate and incommensurate cases. We also compute the momentum distribution of the gas, which is one of the experimentally accessible observables.

The paper is organized as follows. In Sec. II, we introduce the model and the respective physical observables and give the low-energy description of the system via the bosonization approach. Section III describes the numerical DMRG method. The results for the phase diagram both for noninteger and integer filling at varying the strength of the second lattice are given in Sec. IV. Here also the evolution of the Mott lobes with pseudodisorder is given. In Sec. V, we analyze the momentum distribution function and describe its characteristics for a weakly interacting Bose gas within perturbation theory in the strength of the second lattice. In Sec. V, the dependence of the Luttinger exponent on pseudodisorder is also determined. Finally, in Sec. VI we give a summary and the conclusions.

II. MODEL

We consider a one-dimensional Bose gas at zero temperature subjected to a bichromatic lattice potential $V(x)=V_1 \sin^2(k_1 x)+V_2 \sin^2(k_2 x)$,

$$H=\int_{-\infty}^{\infty} dx \psi_b^\dagger(x)\left(-\frac{\hbar^2}{2m}\nabla^2+V(x)\right)\psi_b(x) + \frac{g}{2}\int_{-\infty}^{\infty} dx \psi_b^\dagger(x)\psi_b^\dagger(x)\psi_b(x)\psi_b(x), \quad (1)$$

where $\psi_b(x)$ is the bosonic field operator, m is the atomic

mass, and g represents the contact interaction. In the case in which the main lattice is quite large, i.e., $V_1 \geq E_R$, where $E_R=\hbar^2k_1^2/2m$ is the recoil energy, we can map the system on a Bose-Hubbard model,

$$H = -t\sum_{i=1}^{N_{\text{sites}}-1}(b_i^\dagger b_{i+1}+\text{H.c.}) + \frac{U}{2}\sum_{i=1}^{N_{\text{sites}}} n_i(n_i-1) - \mu\sum_{i=1}^{N_{\text{sites}}} n_i + \sum_{i=1}^{N_{\text{sites}}}\Delta_i n_i, \tag{2}$$

where $b_i^\dagger, b_i$ are bosonic field operators on the site i, t is the hopping amplitude, U is the on-site interaction, μ is the chemical potential, N_{sites} is the total number of lattice sites; and the parameters U,t are related to those of the continuum model (1) (e.g., see Refs. [33,34]). The effect of the second lattice is to induce a modulation of the on-site energies according to $\Delta_i=\Delta\cos(2\pi\alpha i)$, with $\Delta\propto V_2$ the relative strength of the second lattice, and the value of $\alpha=k_2/k_1$ [35] has been chosen as $\alpha=830/1076\approx 0.77$, being the same as that of the experiment in Florence [21].

In order to characterize the different phases of the system, we evaluate the following observables: (i) the superfluid fraction,

$$f_s = \frac{N_{\text{sites}}^2}{Nt\pi^2}(E^N_{\text{antiPBC}} - E^N_{\text{PBC}}), \tag{3}$$

where N is the particle number, and $E^N_{\text{(anti)PBC}}$ is the ground-state energy with (anti)periodic boundary conditions, and (ii) the compressibility, $\chi=(1/L)dN/d\mu$, i.e.,

$$\chi^{-1} = L[E(N+1)+E(N-1)-2E(N)], \tag{4}$$

where L is the length of the chain and E is the ground-state energy.

We also evaluate the momentum distribution as the Fourier transform of the one-body density matrix,

$$n(q) = \mathcal{N}\sum_{lm} e^{iq(l-m)a}\langle b_l^\dagger b_m\rangle, \tag{5}$$

with $a=\pi/k_1$ being the primary lattice spacing and $\mathcal{N}$ a normalization constant.

A. Low-energy properties and bosonization

We focus now on the regime $\Delta \ll 2t$, which is expected to be nonlocalized [23,25,36]. In these conditions, we describe the one-dimensional interacting bosonic fluid as a Luttinger liquid, using a low-energy hydrodynamic description [13,37,38]. In particular, the system is characterized by a slow, power-law decay of the phase-phase correlation function (hence the denomination of "superfluid phase") with an exponent that depends on the interaction parameters.

The low-energy Hamiltonian for the fluid can be written as [13,37]

$$H_0 = \frac{1}{2\pi}\int dx\left(\frac{v_s}{K}[\nabla\phi(x)]^2 + v_sK[\pi\Pi(x)]^2\right). \tag{6}$$

This Hamiltonian is a standard sound wave one in which the fluctuations of the phase $\phi(x)$ represent the phonon modes of the density wave as given by

$$\rho(x) = \left(\rho_0 - \frac{1}{\pi}\nabla\phi(x)\right)\sum_{p=-\infty}^{\infty} e^{i2p[\pi\rho_0 x-\phi(x)]}, \tag{7}$$

where ρ_0 is the average density of particles. The field $\theta(x)=\pi\int' dx'\Pi(x')$ is conjugate of $\phi(x)$, $[\frac{1}{\pi}\nabla\phi(x),\theta(x')] = -i\delta(x-x')$, and represents the phase of the superfluid. The parameters K and v_s used in Eq. (6) are related to the microscopic compressibility and superfluid density through the relations $Kv_s=\pi\rho_s/m$ and $v_s/K=1/\pi\chi$. In the case of contact interaction between bosons $g\delta(x)$ and in the absence of the lattice potential, the Luttinger parameters v_s and K are obtained by the exact solution of the Lieb-Liniger model [38]: $v_sK=\frac{\pi\rho_0}{m}$, as follows from Galilean invariance, and $\frac{v_s}{K}=\frac{g}{\pi}$ in the weak-coupling limit, while $\frac{v_s}{K}=\frac{\pi\rho_0}{m}(1-\frac{8\rho_0\hbar^2}{mg})$ in the strong coupling, $\rho_0=N/L$ being the particle density. The Hamiltonian (6) is an effective low-energy theory [37] and provided that the correct values of the parameters v_s,K are used, all long-wavelength properties of the correlation functions of the system can then be obtained exactly. In the $g=\infty$ limit, i.e., for hard-core bosons, one obtains $K=1$ as for free spinless fermions while the free bosons limit would correspond to $K\to\infty$.

In the low-energy hydrodynamic description, the bosonic field operator can be represented as

$$\psi_B(x) = e^{i\theta(x)}\sqrt{\rho(x)}. \tag{8}$$

The corresponding one-body density matrix $G(x,x',0) = \langle\psi_B^\dagger(x)\psi_B(x')\rangle$ in the long-wavelength limit can be computed [13] and has a power-law decay given by $\sim 1/|x-x'|^{1/2K}$ in the limit of the system size $L\to\infty$. Notice that the knowledge of the compressibility and of the one-body density matrix offers two independent ways of extracting the Luttinger exponent [29] K.

B. Perturbative treatment of the quasiperiodic potential

For the model (6) we are interested in the effect of a bichromatic lattice potential $V(x)=\Sigma_{i=1}^2 V_i\cos(2k_ix)$. We will work in the limit where the strength of both potentials is small with respect to the bandwidth, so that bosonization is applicable. Then, each component V_i of the potential couples to the density and adds a term to the Hamiltonian (6), which reads

$$H_{bl} = V_i\int dx\cos(2k_ix)\rho(x) = \sum_{p=-\infty}^{\infty}\frac{\rho_0V_i}{2}\int dx\cos[(2\pi p\rho_0\pm 2k_i)x - 2p\phi(x)]. \tag{9}$$

Since the field $\phi(x)$ is a slowly varying function on the scale of the interparticle distance, if oscillating terms remain

in the integral, they will average out, leading to a negligible contribution. Therefore, the Luttinger-liquid (superfluid) behavior will persist provided that the filling is not commensurate, i.e., neither of the two commensurability conditions $p\rho_0 \pm k_i/\pi \in \mathbb{Z}$ is satisfied.

For commensurate fillings, i.e., when one of the two commensurability conditions is met, the periodic potential changes the simple quadratic Hamiltonian (6) of the Luttinger liquid into a sine-Gordon Hamiltonian, which describes the Mott transition as a function of interaction strength [13]. Indeed, under the renormalization-group (RG) flow, the operator (9) is irrelevant for $K > K_c = 2/p^2$ and relevant for $K < K_c$, thus implying a Mott-insulator phase at $K < K_c$. As K is decreasing when interactions are made more repulsive, this means that the Mott state is obtained when repulsion exceeds a critical value U_c. In the case in which the Mott insulator is obtained for $p=1$, in the regime of $K < K_c$, none of the terms associated with the second potential (which is incommensurate) can become relevant. Therefore, in that case, for $K > K_c$, the Luttinger liquid is stable, and no Bose-glass phase can be created by the other potential in the vicinity of the Mott-insulator superfluid transition in the regime where bosonization is applicable. This justifies the shape of the phase diagram of Fig. 1 for the commensurate case. The renormalization group analysis shows that the transition from the Mott insulator to the superfluid belongs to the Kosterlitz-Thouless universality class [13]. Note that the term (9) has been derived here for a weak lattice potential, but it appears also in the opposite limit of a strong lattice potential if the filling is commensurate, showing that the two limits are smoothly connected [13].

A different situation occurs in the case of random distributed disorder. As shown in Ref. [3], the potential becomes relevant below the critical value $K_c = 3/2$. Below such a value, the system lies in a Bose-glass phase with an exponentially decaying Green's function on the scale of the localization length. A detailed RG analysis for the case of a generic quasiperiodic potential was given in Refs. [41,42]. There it was shown that in the case in which the quasiperiodic potential has a nontrivial, dense Fourier spectrum, the critical value of K_c can be actually smaller than the value $K_c = 2$, the deviation from $K_c = 2$ being related to the distance of $2\pi\rho_0$ to a harmonic of the Fourier transform of the potential, thus interpolating between the two-color potential and the fully random case.

If we now consider the phase transition between the Mott state and the superfluid, not as a function of interaction, but as a function of particle density or as a function of the chemical potential, it is well known that in the absence of the secondary lattice potential, this is a commensurate-incommensurate (C-IC) transition [13,33,39,40]. At the transition, the scaling dimension of the operator $\cos 2\phi$ associated with the main lattice potential must be 1, which yields $K_c = 1$. Turning on a second, weak lattice potential incommensurate to the first, we see that the problem is reduced to free fermions in a bichromatic lattice. The rigorous results on the Harper model [25] then indicate that for a potential that is small compared with the bandwidth, the states are not localized by the incommensurate potential. Therefore, a weak incommensurate potential cannot turn the superfluid state formed by doping the Mott insulator in a Bose-glass state. Again, this is at variance with the effect of the random potential, which would immediately localize the particles as the Mott gap closes. With model (2), in the limit of very strong repulsion $U \gg t$, and for a filling slightly below one particle per site, we can also use the Harper model mapping to predict that the Bose glass to superfluid transition will happen when $\Delta = 2t$. Thus, in the phase diagram at fixed U, and varying t, we expect that wings of a Bose-glass phase will be obtained for sufficiently small t. Summarizing the results for the Mott transition as a function of chemical potential and interaction, we expect in the two-color potential a scenario similar to the scenario 2(c) in [2], i.e., that near the tip of the Mott lobe there is no Bose-glass phase in the case of the two-color potential, provided that the incommensurate potential is small compared to the bandwidth.

III. NUMERICAL METHOD

In order to determine the ground-state properties of the interacting Bose gas in the bichromatic lattice, we use the density matrix renormalization group (DMRG) method [14,15]. The DMRG is a quasi-exact numerical technique widely employed for studying strongly correlated systems in low dimensions. Based on the renormalization, it finds efficiently the ground state of a relatively large system with quite high precision. Recently, the DMRG was used to study the one-dimensional (1D) disordered Bose-Hubbard model [43].

We consider a system with periodic boundary conditions and use first the infinite-size algorithm to build the Hamiltonian up to the length L, then we resort to the finite-size algorithm to increase the precision within many sweeps. In principle, the Hilbert space of bosons is infinite; to keep a finite Hilbert space in the calculation, we choose the maximal number of boson states approximately of the order $5\langle n\rangle$, varying $n_{\max}$ between $n_{\max}=6$ and 15, except close to the Anderson localization phase where we choose the maximal boson states $n_{\max}=N$. The number of eigenstates of the reduced density matrix are chosen in the range 80–200. To check the error produced by truncating the boson space, we have repeated the calculations at varying $n_{\max}$ in the range $5\langle n\rangle$ and $10\langle n\rangle$, without observing a substantial difference in the ground-state energy. To test the accuracy of our DMRG method, in the case $U=0$ or for finite U and small chain, we have compared the DMRG numerical results with the exact solution obtained by direct diagonalization. For a larger system ($N_{\text{sites}} > 10$), we have checked the convergence of the ground-state energy by varying the number of truncated eigenstates, estimating that in the region of the superfluid-Mott insulating phase, the errors are of the order 10^{-6}. The good convergence of the algorithm is also tested by the coherence of the results obtained from different observables as the Mott-insulator density plateaus and correlation functions [44].

The calculations are performed in the canonical ensemble, i.e., at a fixed number of particles N. The chemical potential is determined by the evaluation of the energy required to add or subtract a particle to the ground state, i.e., $\mu^p = E(N+1)$

$-E(N)$ and $\mu^h=E(N)-E(N-1)$ [16]. In this way, we may obtain the phase diagram in the grand-canonical ensemble. In order to find the superfluid density and the compressibility at varying chemical potential, we performed several calculations at varying particle numbers. For the determination of the phase diagram, we have chosen $N_{\text{sites}}=20$, while the correlation functions have been calculated using a larger chain $N_{\text{sites}}=50$.

IV. PHASE DIAGRAMS

We have determined the phase diagram in two situations. First, we have analyzed the effect of interactions on the localization and delocalization threshold with respect to its noninteracting value $\Delta=2t$ obtained from the Harper model [23] or equivalently for the hard-core Bose gas. Second, we have analyzed the effect of disorder on the Mott-insulator lobes [2].

A. Localization and delocalization transition

1. Incommensurate filling: Case $\langle n\rangle=1/2$

By the calculation in the canonical ensemble of the superfluid fraction and of the compressibility, we have mapped the phase diagram in the plane $(\Delta/t, U/t)$. This is illustrated in Fig. 3(a) by showing the contour plot of the superfluid fraction obtained for $N_{\text{sites}}=20$. In the case of noninteger filling, only two types of phase are present: a superfluid phase ($f_s\neq 0$) at small values of the secondary lattice height Δ (bottom left), and a glass phase ($f_s=0$) at large values of Δ for $\Delta>U$ (top left). At $U=0$, the transition occurs at the expected critical value $\Delta/t=2$. For $U\to\infty$, the critical value of $\Delta/t=2$ is also recovered. We see that at intermediate values of the interaction strengths U, the critical value of Δ_c/t increases and there the superfluid region extends in a large dome. A similar behavior is observed for a disordered Bose gas [3]. The top-right corner of the phase diagram is also formed by a glass phase. Using only the superfluid fraction, it is not possible to distinguish the two possible glass phases, Anderson glass and Bose glass, since they are both characterized by a nonzero compressibility and a zero superfluid fraction. However, in the Anderson glass phase, the average density is expected to be highly inhomogeneous [3] as all bosons condense in the lowest localized state, while in the Bose glass, because of the interparticle repulsion, the average density is more homogeneous. In order to contrast the two phases, we have plotted in Fig. 2 the density profile for two different values of U at fixed t and Δ. For $U=0$ [top-left corner of Fig. 3(a)], the Anderson glass is obtained, with a density profile highly peaked on a few sites (see the main panel of Fig. 2). By contrast, for $U=5$ [top-right corner of Fig. 3(a)], the density becomes much more homogeneous (inset of Fig. 2). Let us note that there is no actual phase transition between the Bose glass and the Anderson glass, but rather a gradual crossover. Thus, the glass phase obtained for small U in Fig. 3(a) will present an Anderson glass character, while the phase obtained for large U will present a Bose-glass character, but changing the interaction U gradually allows it to pass from one phase to the other without any discontinuity, as shown in the main panel of Fig. 2.

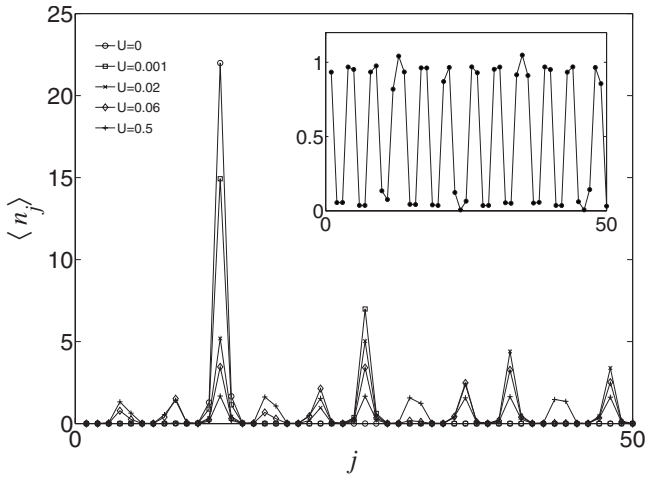

FIG. 2. A plot of the density profile for half-filling $(L=50, N=25)$, showing the evolution from the Anderson-glass phase toward the Bose-glass phase. The main frame is showing the density profile starting from the Anderson glass at increasing interaction U, while the inset shows the Bose-glass density profile. The parameters are $t=0.5, \Delta=2, U=0$ (circles), $U=0.001$ (squares), $U=0.02$ (diagonal crosses), $U=0.06$ (diamonds), $U=0.5$ (crosses), and $t=0.5, \Delta=2, U=5$ for the Bose glass in the inset.

2. Commensurate filling: Case $\langle n\rangle=1$

The phase diagram for the integer filling is given in Fig. 3(b), where we show the superfluid fraction f_s (main figure) and the compressibility gap $(\mu^p-\mu^h)/t$ (inset) obtained for $N_{\text{sites}}=20$. The Mott phase, which is characterized by a large compressibility gap, emerges at the bottom-right corner above the critical value $U_c/t=3.3\pm 0.2$ for $\Delta=0$, in agreement with Refs. [29,30]. We observe that U_c increases at increasing Δ, meaning that disorder energetically reduces the compressibility gap in the localized regime [see also Fig. 4(a)]. A glass phase instead occurs in the region of the phase diagram $\Delta>U$ (top left). At $U=0$, the transition occurs at the expected value $\Delta_c/t=2$. The critical value of Δ_c increases with U at small U, indicating a delocalization by interactions, similarly to the true-disorder case. Finally, a superfluid phase emerges in the small U and small Δ region of the phase diagram (bottom left). In our simulations, it extends in a large dome at intermediate U and Δ. The behavior of the superfluid fraction and compressibility gap for small Δ and intermediate U seems to indicate a direct transition from the superfluid to the Mott-insulating state without passing into a Bose glass. Such a conclusion seems physically reasonable if one takes into account that the bichromatic lattice potential acts as a quasidisorder, i.e., is less relevant than true disorder. Anyway, such a conclusion should be supported by further numerical investigation and finite-size scaling of the compressibility and superfluid fraction. Concerning the nature of the glass phase, whether Anderson or Bose type, the same

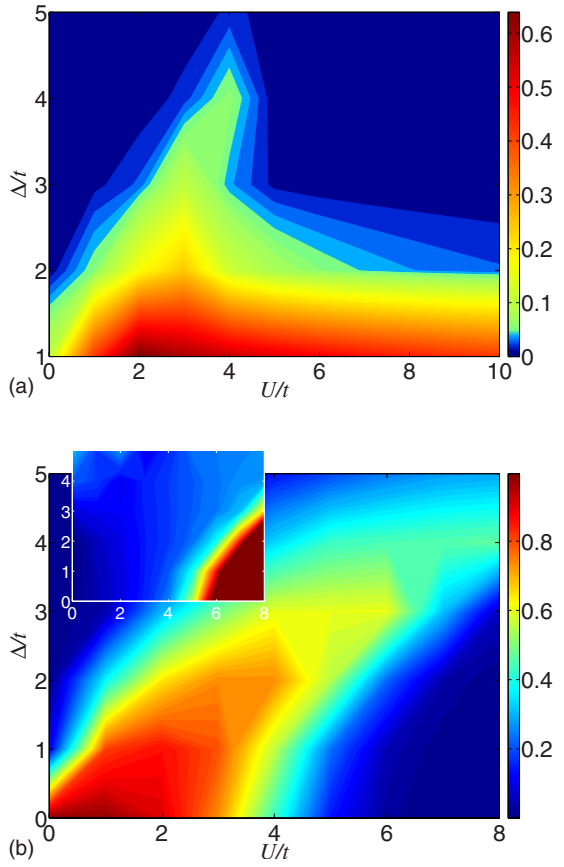

FIG. 3. (Color online) DMRG phase diagram for an interacting Bose gas in a two-color lattice, in the plane $(\Delta/t,\ U/t)$. (a) Superfluid fraction in the case of noninteger filling $\nu=N/N_{\text{sites}}=0.5$, with $N=10$, $N_{\text{sites}}=20$. (b) The superfluid fraction f_s (main figure) and compressibility gap $(\mu^p-\mu^h)/t$ (inset) in the case of integer filling with $N=N_{\text{sites}}=20$.

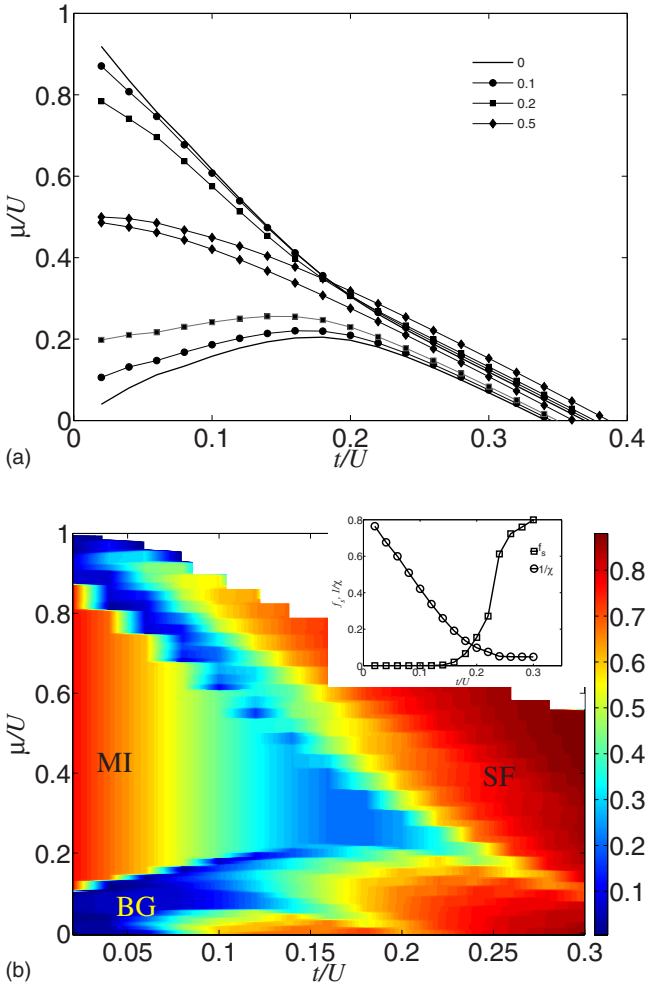

FIG. 4. (Color online) DMRG phase diagram for an interacting Bose gas in a two-color lattice, in the plane $(\mu/t,\ t/U)$, for the first Mott lobe, for $N=N_{\text{sites}}=20$. (a) The shrinking of the Mott lobe at varying $\Delta/U=0$ (solid line), 0.1 (circles), 0.2 (squares), and 0.5 (diamonds). (b) Contour plot of the function $f_s+(\mu^p-\mu^h)/t$ for $\Delta/U=0.1$. The inset shows the compressibility gap $(\mu^p-\mu^h)/t$ and the superfluid fraction f_s along the line $\mu/U=0.25$.

remarks apply as in the incommensurate case discussed in Sec. IV A 1, namely the two phases are distinguished only by the inhomogeneity of their density profile, and one can go continuously from the Anderson to the Bose glass simply by increasing the repulsion.

B. Mott-insulator lobes

We have performed the calculation of the Mott-insulator lobes in the grand-canonical ensemble. This is obtained by the estimation of μ^p and μ^h for several values of particle numbers. At increasing strength of the second lattice, we find that the Mott-insulator lobe with $\langle n\rangle=1$ shrinks and finally tends to disappear for $\Delta\sim 0.5$, as is illustrated in Fig. 4(a). In order to determine the Bose-glass region, we have also calculated the superfluid density. Figure 4(b) shows, for a specific choice of Δ, the regions of nonzero superfluid density as well as the regions of large compressibility gap (Mott-insulator phase) through the function $f_s+(\mu^p-\mu^h)/t$. The intermediate (dark blue) region between the two corresponds to the Bose-glass phase. Notice that near the tip of the Mott lobe, the superfluid fraction is nonzero, as illustrated in the inset of Fig. 4(b), supporting the direct superfluid to Mott-insulator transition, discussed above. We also notice in Fig. 4 the presence of a Bose-glass phase for $t/U\leq\Delta/2U$, as expected from the strong-coupling argument.

V. MOMENTUM DISTRIBUTION

A. Side peaks of the momentum distribution

The results for the momentum distribution are reported in Fig. 5. We note that besides the expected peak of the momentum distribution at $k=0$, there are other peaks at $k=\pm Q=\pm\frac{2\pi}{a}(1-\alpha)$ related to the modulation of the on-site energy in Eq. (2). The origin of these peaks can be understood by considering first noninteracting bosons. We will begin by discussing the continuum limit, and then the lattice case. If we approximate the irrational number α [35] by a rational number p/q, in the potential $V(x)$, we can apply Bloch's theorem and write the boson annihilation operator as

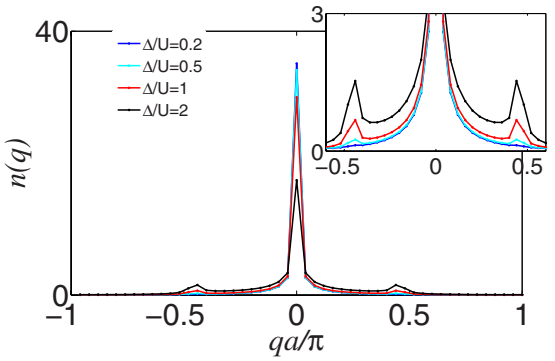

FIG. 5. (Color online) DMRG momentum distribution function in the superfluid phase at varying Δ/U (as indicated in the figure) and $U=2t$, with $N=N_{\text{sites}}=50$. Subdominant peaks are determined by the presence of the second lattice potential (see text).

$$\hat{\psi}_b(x) = \frac{1}{\sqrt{N}} \sum_k \sum_{\beta=1}^{q} e^{ikx} \varphi_k^{(\beta)}(x) b_{k,\beta}, \tag{10}$$

where k is the quasimomentum of the boson and β is the band index. Bose condensation will then occur in the lowest quasimomentum state of the lowest band (we chose $\beta=1$ for this band). The functions $\varphi_k^{(\beta)}(x)$ are periodic of period qa, i.e., $\varphi_k^{(\beta)}(x)=\varphi_k^{(\beta)}(x+qa)$. Using this property, one finds that in the Bose-condensed state, $\langle \psi_b^\dagger(x+qa)\psi_b(x'+qa)\rangle = \langle \psi_b^\dagger(x)\psi_b(x')\rangle$. As a result, after averaging over x, the function $\langle \psi_b^\dagger(x+r)\psi_b(x)\rangle$ becomes a periodic function of r of period qa. Using Fourier transformation, we conclude that the states of momentum $(2\pi/a)(\pm 1/q+M)$, where $M \in \mathbb{Z}$, present a macroscopic occupation number. If we turn to perturbation theory, in the limit of $\Delta \ll t$, we find that the perturbed wave function at the lowest order is given by

$$\varphi_k^{(1),1}(x) = \varphi_k^{(1),0}(x) + \sum_{Q,m} \frac{\varphi_k^{(m),0}(x)}{E_{Q,m} - E_{k,1}} \langle \varphi_k^{(m),0}(x)| V_2 \cos(2\alpha k_1 x) \times |\varphi_k^{(1),0}(x)\rangle, \tag{11}$$

where $\varphi_k^{(m),0}(x)$ are the solutions of a Mathieu equation [45] for the potential $V_1 \cos(2k_1 x)$ and $E_{Q,n}$ is the dispersion of the nth band for momentum Q. The matrix elements of perturbation are nonzero only when $Q=Q_\pm=(2\pi/a)(\pm\alpha+M')$ $(M' \in \mathbb{Z})$.

The momentum distribution is then given by $n(p) = \left|\int dx e^{ipx} \varphi_{k=0}^{(1),1}(x)\right|^2$, and using Eq. (11) we find that it displays two peaks,

$$n(p) \sim |\varphi_0^0(p)|^2 + \sum_{\delta=\pm} \left| \frac{V_2}{E_{Q_\delta} - E_0} \right|^2 |\varphi_0^0(p+Q_\delta)|^2, \tag{12}$$

where [45] $\varphi_0^0(p) \propto e^{-p^2/p_0^2}$ and $p_0 = \frac{\pi}{a}\left(\frac{E_R}{8V_1}\right)^{1/4}$.

In an analogous way, we can proceed to derive the expression for the momentum distribution on the lattice. The perturbed boson annihilation operator is then

$$b_k = b_k^{(0)} + \sum_{\delta=\pm} \frac{\Delta}{-2t\{\cos[(k+Q_\delta)a] - \cos(ka)\}} b_{k+Q_\delta}^{(0)}, \tag{13}$$

so that the largest occupation number will be found for $k=0$, and again at $k=Q_\pm$ (modulo the reciprocal-lattice vector). The physical interpretation of the extra peaks is therefore that the ground-state wave function is diffracted by the quasiperiodic potential, thus creating peaks at multiple harmonics of $2\pi\alpha/a$ (modulo a vector of the reciprocal lattice).

Let us now turn to the case of weakly interacting bosons. If the repulsion U is not too large, we can still begin by diagonalizing the noninteracting Hamiltonian, and treat the interaction within a Bogoliubov approximation or numerically solve the Gross-Pitaevskii equation [46]. Since Bose condensation is obtained in the lowest band, it is reasonable to neglect the contribution from the higher bands. Moreover, since the states that are important for the low-energy properties are those with quasimomentum near zero, we can neglect the dependence of $\varphi_k^{(1)}(x_i)$ on k. This gives us the following expression for the boson annihilation operator [47]:

$$b_i \simeq \varphi_0^{(1)}(x_i) \tilde{b}_i, \tag{14}$$

where $\tilde{b}_i = \frac{1}{N^{1/2}} \Sigma_k e^{ikx_i} b_{k,1}$. Injecting this approximation in the full Hamiltonian, we obtain an interaction term that has the same period q as the potential Δ_i. This gives rise to new umklapp processes, but since we are only interested in the states of momenta close to zero, we can neglect them. Then, the theory describing the $\tilde{b}$ bosons becomes identical to the one describing bosons in the absence of an incommensurate potential, albeit with a dispersion fixed by the band structure and an interaction $U_{\text{eff}} = U\Sigma_{i=0}^{q-1} |\varphi_0^{(1)}(x_i)|^4/q$.

The single-particle density matrix is

$$\langle b_i^\dagger b_j \rangle = [\varphi_0^{(1)}(x_i)]^* \varphi_0^{(1)}(x_j) \langle \tilde{b}_i^\dagger \tilde{b}_j \rangle, \tag{15}$$

and thus the effect of the periodic potential is only seen in the appearance of the factor $[\varphi_0^{(1)}(x_i)]^* \varphi_0^{(1)}(x_j)$. Using the bosonization technique to compute the single-particle density matrix $\langle \tilde{b}_i^\dagger \tilde{b}_j \rangle$, we finally find that

$$\langle b_i^\dagger b_j \rangle = \frac{[\varphi_0^{(1)}(x_i)]^* \varphi_0^{(1)}(x_j)}{|i-j|^{1/(2K)}}. \tag{16}$$

By Fourier transforming the above expression, we recover power-law peaks in the momentum distribution with exponent $[1/2K-1]$ for all the wave vectors that are multiples of $2\pi/qa$. Based on the previous perturbation theory, we expect that the two subleading peaks will be found at $k=(2\pi/a)(m \pm p/q)$ with $m \in \mathbb{Z}$. Moreover, the exponent should be identical to the one found for $q=0$. We also remark that if the peaks were produced by the terms $e^{i2\pi\rho_0 x} e^{i(\theta-2\phi)}$ in the expansion of the boson annihilation operator (8), their position would depend on the number of particles per site, and their height would be independent of the strength of the incommensurate potential. Moreover, these terms give in real space a correlation function of the form $(|x-x'|/\alpha)^{-(2K+1/2K)}$ with an exponent that is always larger than 2. As a result, the Fourier transform of this term would not diverge as

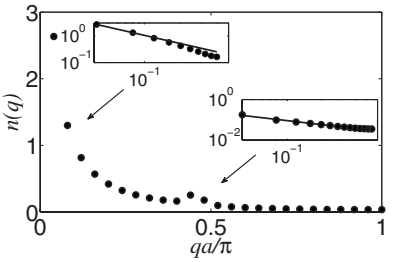

FIG. 6. Fourier transform of DMRG momentum distribution function in the superfluid phase with $\Delta=0.5U$, $U=2t$, and $N=N_{\text{sites}}=50$. The main peak and the subdominant one decay with a power-law exponent consistent with $[1/2K-1]\sim 0.85$ for q sufficiently close to 0 and $2\pi(1-\alpha)/a$ as shown in log scale in the insets.

$k\rightarrow(2\pi/a)(m\pm p/q)$, rather a cusp could be obtained.

We have checked that the height of the secondary peak increases quadratically with the strength of the incommensurate potential as expected from Eq. (12), that its position does not change with the filling, and that it possesses the same power-law divergence as the peak obtained at $k=0$. This is shown in Fig. 6, where the Fourier transform of the momentum distribution is displayed together with the power-law decay of the peak at $q=0$ and of the satellite peak in a log scale.

B. Determination of the Luttinger exponent

According to Eq. (16), in the superfluid phase the one-body density matrix $\rho_1(i,j)=\langle b_i^\dagger b_j\rangle$ can be used to extract the Luttinger exponent K. This is particularly interesting because, even though bosonization techniques do not directly access the localized phase, the fact that the Luttinger exponent K depends on the strength Δ of the pseudodisorder indicates a first disruption of the superfluid phase toward localization. In order to analyze the DMRG data for the one-body density matrix, we take into account both the density modulation induced by the second lattice [entering explicitly in Eq. (16) through the factors $\varphi_0(x_i)$] and the fact that the calculations are performed on a system of finite length L. For the latter case, we use the results of the continuum model obtained by using the conformal field theory [38] for a system of length L and periodic boundary conditions. In essence, we fit the DMRG results by the following expression:

$$\rho_1(j,0)=\sqrt{n_0+\delta\cos[2\pi(1-\alpha)j+\phi_0]}\left(\frac{1}{d(\,ja|L)}\right)^{1/2K}, \tag{17}$$

where n_0, δ, and ϕ_0 are constants, K is the Luttinger parameter, and d is the conformal length $d(\,x|L)=\frac{L}{\pi}|\sin(\frac{\pi x}{L})|$. The results are shown in Fig. 7. By the fit, we obtain that the Luttinger exponent K decreases at increasing Δ, in agreement with the intuition that disorder drives the system toward a more correlated, less superfluid phase. The corresponding values are reported in Table I.

Another independent way to extract K is based on the determination of the ground-state energy and compressibility

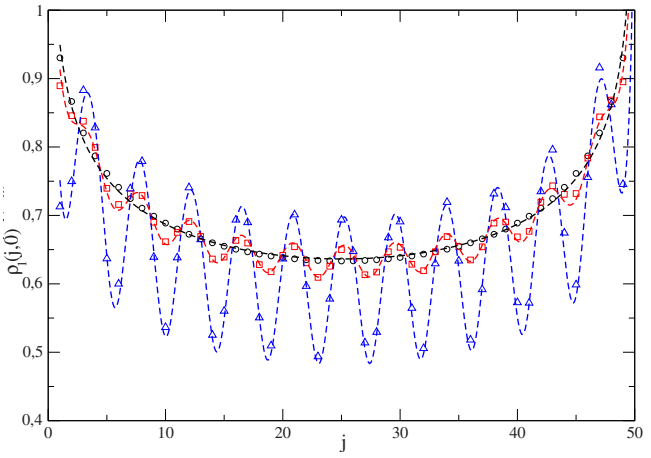

FIG. 7. (Color online) One-body density matrix from DMRG data ($\Delta/U=0$ circles, $\Delta/U=0.1$ squares, $\Delta/U=0.5$ triangles) and from fit to Eq. (17) (dashed lines). The parameters used are $U=2t$ and $N=N_{\text{sites}}=50$.

χ given by Eq. (4), by the relation $K=\hbar\pi\sqrt{\rho_s\chi/m}$. We have verified that the values of K extracted in this way are consistent with those of Table I.

VI. SUMMARY AND CONCLUDING REMARKS

We have analyzed the phase diagram of an interacting one-dimensional Bose gas in the presence of a pseudodisorder generated by a bichromatic lattice potential. Starting from a Bose-Hubbard model, we have considered both commensurate and incommensurate fillings and we have found a rich phase diagram including, in addition to the superfluid and Mott phases, a Bose-glass phase, localized but compressible. In agreement with the limiting cases of free and hard-core bosons described by an almost Mathieu problem, the transition toward the Bose glass phase is found at $\Delta/t\geq 2$, the critical value of Δ being higher for bosons with finite interaction strength. This nonmonotonic dependence of the critical height of the second lattice on the interaction strength could be observed in the experiments. We have also analyzed the shrinking of the Mott lobes as a function of Δ and the emergence of a Bose-glass phase in the $(\mu/U,t/U)$ plane. Finally, we have characterized the superfluid phase by a static observable, the momentum distribution function. We have shown that satellites peaks emerge when the pseudodisorder is not too strong and their interpretation within perturbation theory offers a good qualitative understanding of their behavior as a function of the height of the second lat-

TABLE I. Values of the Luttinger exponent from the fit of the DMRG data to Eq. (17) with the parameters of Fig. 7. The corresponding χ^2 is of the order of 5×10^{-5}.

Δ/U	K
0.0	3.44 ± 0.03
0.1	3.43 ± 0.04
0.5	3.35 ± 0.06

tice. The central peak of the momentum distribution allows us to determine the Luttinger exponent K, whose knowledge is useful to make predictions for further physical quantities.

While the momentum distribution and the behavior of the side peaks could characterize the evolution of the system toward a Bose glass, a direct probe of a Bose glass phase and its distinction from a Mott insulator could be provided by study of noise correlations or collective excitations. This will be left for future study.

Note added: Recently, we became aware of a related work by Roux *et al.* [48].

ACKNOWLEDGMENTS

R.C. acknowledges financial support from a Marie-Curie Intra-European grant. We thank Professor T. Giamarchi for comments on our manuscript.

[1] P. W. Anderson, Phys. Rev. **109**, 1492 (1958).
[2] M. P. A. Fisher, P. B. Weichman, G. Grinstein, and D. S. Fisher, Phys. Rev. B **40**, 546 (1989).
[3] T. Giamarchi and H. J. Schulz, Phys. Rev. B **37**, 325 (1988).
[4] M. H. W. Chan, K. I. Blum, S. Q. Murphy, G. K. S. Wong, and J. D. Reppy, Phys. Rev. Lett. **61**, 1950 (1988).
[5] G. K. S. Wong, P. A. Crowell, H. A. Cho, and J. D. Reppy, Phys. Rev. Lett. **65**, 2410 (1990).
[6] A. van Oudenaarden, S. J. K. Várdy, and J. E. Mooij, Phys. Rev. Lett. **77**, 4257 (1996).
[7] W. Krauth, N. Trivedi, and D. Ceperley, Phys. Rev. Lett. **67**, 2307 (1991).
[8] S. Zhang, N. Kawashima, J. Carlson, and J. E. Gubernatis, Phys. Rev. Lett. **74**, 1500 (1995).
[9] F. Alet and E. S. Sorensen, Phys. Rev. B **70**, 024513 (2004).
[10] P. Hitchcock and E. S. Sorensen, Phys. Rev. B **73**, 174523 (2006).
[11] I. M. Lifshitz, L. P. Pastur, and S. Gredeskul, *Introduction to the Theory of Disordered Systems* (Wiley, New York, 1988).
[12] N. F. Mott and A. D. Twose, Adv. Phys. **10**, 107 (1961).
[13] T. Giamarchi, *Quantum Physics in One Dimension* (Oxford University Press, Oxford, 2004).
[14] S. R. White, Phys. Rev. Lett. **69**, 2863 (1992); Phys. Rev. B **48**, 10345 (1993).
[15] U. Schollwöck, Rev. Mod. Phys. **77**, 259 (2005).
[16] G. G. Batrouni and R. T. Scalettar, Phys. Rev. B **46**, 9051 (1992).
[17] B. V. Svistunov, Phys. Rev. B **54**, 16131 (1996); N. V. Prokof'ev and B. V. Svistunov, Phys. Rev. Lett. **80**, 4355 (1998).
[18] J. K. Freericks and H. Monien, Phys. Rev. B **53**, 2691 (1996).
[19] P. Schmitteckert, T. Schulze, C. Schuster, P. Schwab, and U. Eckern, Phys. Rev. Lett. **80**, 560 (1998).
[20] M. Greiner, O. Mandel, T. Esslinger, T. W. Hänsch, and I. Bloch, Nature (London) **415**, 39 (2002).
[21] L. Fallani, J. E. Lye, V. Guarrera, C. Fort, and M. Inguscio, Phys. Rev. Lett. **98**, 130404 (2007).
[22] J. E. Lye, L. Fallani, C. Fort, V. Guarrera, M. Modugno, D. S. Wiersma, and M. Inguscio, e-print arXiv:cond-mat/0611146.
[23] P. G. Harper, Proc. Phys. Soc., London, Sect. A **68**, 874 (1955); S. Aubry, in *Solitons and Condensed Matter Physics*, edited by A. R. Bishop and T. Schneider (Springer, New York, 1978); S. Aubry and G. Andre, Ann. Isr. Phys. Soc. **3**, 133 (1980); S. Aubry, J. Phys. (Paris) **44**, 147 (1983).
[24] D. R. Hofstadter, Phys. Rev. B **14**, 2239 (1976).
[25] Ya. Svetlana Jitomirskaya, Ann. Math. **150**, 1159 (1999).
[26] M. Girardeau, J. Math. Phys. **1**, 516 (1960); M. D. Girardeau, Phys. Rev. **139**, B500 (1965).
[27] A. M. Rey, I. I. Satija, and C. W. Clark, Phys. Rev. A **73**, 063610 (2006).
[28] C. Schuster, R. A. Romer, and M. Schreiber, Phys. Rev. B **65**, 115114 (2002).
[29] T. D. Kühner and H. Monien, Phys. Rev. B **58**, R14741 (1998).
[30] V. A. Kashurnikov and B. V. Svistunov, Phys. Rev. B **53**, 11776 (1996).
[31] R. Roth and K. Burnett, Phys. Rev. A **68**, 023604 (2003).
[32] T. Roscilde, e-print arXiv:0712.2741.
[33] H. P. Büchler, G. Blatter, and W. Zwerger, Phys. Rev. Lett. **90**, 130401 (2003).
[34] D. Jaksch, C. Bruder, J. I. Cirac, C. W. Gardiner, and P. Zoller, Phys. Rev. Lett. **81**, 3108 (1998).
[35] In the definition of the Harper model [23,25], α is an irrational number. However, to all practical purposes and in numerical calculations it is then approximated by a close rational number.
[36] J. X. Zhong and R. Mosseri, J. Phys.: Condens. Matter **7**, 8383 (1995).
[37] F. D. M. Haldane, Phys. Rev. Lett. **47**, 1840 (1981).
[38] M. Cazalilla, J. Phys. B **37**, S1 (2004).
[39] G. I. Dzhaparidze and A. A. Nersesyan, JETP Lett. **27**, 334 (1978).
[40] H. J. Schulz, Phys. Rev. B **22**, 5274 (1980).
[41] J. Vidal, D. Mouhanna, and T. Giamarchi, Phys. Rev. Lett. **83**, 3908 (1999).
[42] J. Vidal, D. Mouhanna, and T. Giamarchi, Phys. Rev. B **65**, 014201 (2001).
[43] S. Rapsch, U. Schollwöck, and W. Zwerger, Europhys. Lett. **46**, 559 (1999); L. Urba and R. P. Anders, Phys. Rev. B **67**, 104406 (2003).
[44] N. Hatano, J. Phys. Soc. Jpn. **64**, 1529 (1995).
[45] J. C. Slater, Phys. Rev. **87**, 807 (1952).
[46] M. Krämer, C. Menotti, L. Pitaevskii and S. Stringari, Eur. Phys. J. D **27**, 247 (2003).
[47] By following Ref. [46], it can be shown that the functions $\varphi_0^{(1)}$ satisfy Bloch's theorem and give rise to bands, thus an equation equivalent to Eq. (13) can be derived also for weakly interacting bosons.
[48] G. Roux *et al.*, e-print arXiv:0802.3774.